

INCREASING ACCURACY OF ACTIVE POWER MEASUREMENT OF NON-COHERENTLY SAMPLED SIGNALS BY TIME DOMAIN SIGNAL PROCESSING

Martin Novotny¹, Milos Sedlacek¹

¹ Czech Technical University in Prague, Prague, Czech Republic, {SedlacekM, NovotnyM5}@fel.cvut.cz

Abstract: The paper analyses an effective method of increasing accuracy of active power measurement (and energy measurement) by non-coherent sampling. The measurement bias caused by non-coherent sampling are reduced by windowing the instantaneous power sequence of samples by various generalized cosine windows. Active power is found by processing signal in time domain, without using FFT. Newly obtained analytical formulae are given, a comparison to classical method and numerical simulations verifying the derived formulae are presented. A simple method of compensation multiplexing delay by measurement using multiplexing DAQ plug-in board is explained and verified both in simulation and measurement. Application of windowing for measurement of multi-frequency signals is also included, formula for standard uncertainty of active power estimate is given. Basic numerical integration methods applied to quantized input signals in power computation are briefly compared, and numerical values showing decrease in power bias for selected windows are shown.

Keywords: power measurement, DSP, signal windowing.

1. INTRODUCTION

The active power can be found by numerical processing of current and voltage samples, either in time domain or in frequency domain. Classical time-domain algorithms are based on signal period estimation, accuracy of which determines the active power estimation uncertainty. Coherent sampling, i.e. sampling integer number of signal periods, is usually supposed. In case of periodic signals, the fundamental period time of the instantaneous power is half the fundamental period time of the voltage and power. The phase-locked loop (PLL) can be sometimes used to allow the coherent sampling [1]. Coherent sampling is often not provided for in practice. In this case the well known signal “leakage” occurs and windowing and various interpolations are used in DFT if signal is processed in frequency domain [2] - [5]. The detailed analysis of power measurement oriented to up to 3-points interpolated DFT can be found in [6], together with basic information about active power estimation in time domain.

An interesting alternative to windowing by signal processing in frequency domain is the windowing and consecutive signal processing in time domain. This

procedure can be effectively used by measurement of active power and information about its properties is the main topic of this paper.

2. FINDING ACTIVE POWER IN TIME DOMAIN

Active power estimation for analog or digitized signals is based on the relation

$$P' = \frac{1}{T_M} \int_0^{T_M} v(t)i(t)dt \cong \frac{1}{N} \sum_{n=0}^{N-1} v(n)i(n) \quad (1)$$

where P' is active power estimate, T_M is time of measurement (in classical approach one signal period or integer number of the signal periods) and $v(t)$ and $i(t)$ are continuous-time voltage and current, $v(n)$ and $i(n)$ are sequences of voltage and current samples. N is number of acquired samples and there is $T_M = N T_s$, T_s being sampling interval. The measurement time can be expressed also as

$$T_M = (M + \lambda) \cdot T_{sig} \quad (2)$$

where (the positive integer) M is number of integer periods sampled, T_{sig} is the signal period and λ is the decimal part of the last period sampled ($0 \leq \lambda < 1$). There is $P' = P$ for $\lambda = 0$ (coherent sampling), and $P' \neq P$ for $\lambda \neq 0$. The difference between P' and P is the bias of the measured active power P for measurement in time domain caused by non-coherent sampling. The relative bias of P estimation for sinusoidal signal could be expressed as

$$\delta'_p = \frac{P' - P}{P} \quad (3)$$

Using the above given expressions it can re-written as

$$\delta'_p = \frac{\sin[4\pi(M + \lambda)] - \text{tg}\varphi[1 - \cos[4\pi(M + \lambda)]]}{4\pi(M + \lambda)} \quad (4)$$

where φ is the phase of the load impedance (i.e. the phase shift between sinusoidal voltage drop across the load and the load current). The bias is zero for coherent sampling ($\lambda = 0$), and can be surprisingly large for non-coherent sampling for low power factors (because of high value of $\text{tg}\varphi$ in numerator of (4) and by low value of P in (2)).

The dependence of relative bias of active power on the relative time of sampling (time related to signal period) for selected values of the load impedance phase φ is shown in

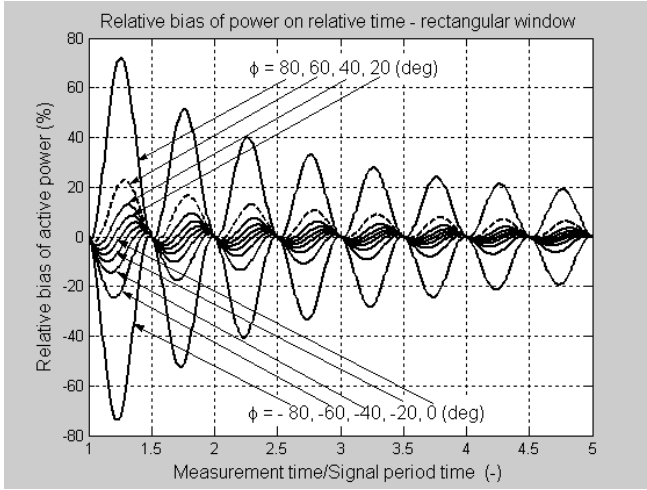


Fig. 1. Bias of active power for rectangular window

Fig.1. Waveforms in this figure are overlapping results of calculation using (4) and computer simulations. Fig.2 shows the same graph as Fig.1, but plotted for relative time from zero to 50 signal periods, to demonstrate the rate of decrease of active power bias for longer times.

An important practical issue is influence of *non-simultaneous sampling* of voltage and current signals. The DAQ PC plug-in boards used in industrial practice are very often “low-cost” multiplexing cards having one common analog-to-digital converter used for all signal input channels. The multiple inputs of the plug-in board are connected to this ADC by means of a multiplexer. The input channels are in this case often sampled by frequency f_s/M , if M input channels of the board are used, and if f_s is the ADC sampling frequency. (This may not be the case of some multiplexing DAQ plug-in boards in regime of much slower sampling rate than the maximum sampling rate of the board). Sampling instants of neighbouring channels are therefore mutually time-shifted by $1/(f_s \cdot M)$ (s).

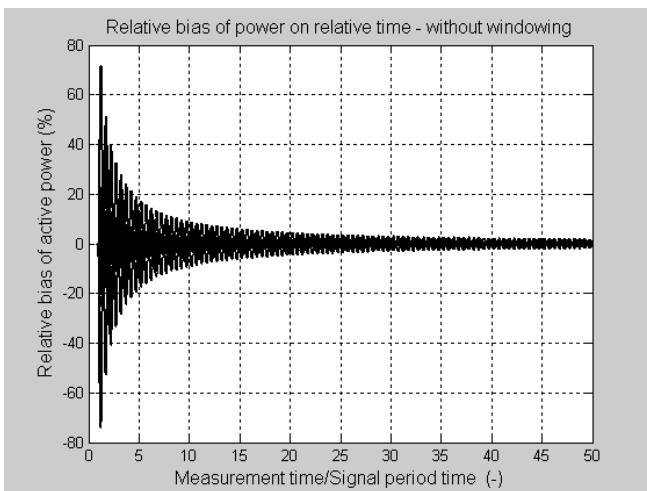


Fig. 2. Bias of active power for rectangular window, load impedance phase-shifts ϕ are the same as in Fig.1

If as in our case there are only two input signals, one corresponding to load voltage and the other one corresponding to load current, these signals are sampled in

time sequences shifted by T_s , where $T_s=1/f_s$ is the sampling interval of the plug-in board ADC. Sampling frequency of both inputs is $f_{si} = f_s/2$. This time shift between voltage and current causes additional power estimate bias, depending on ratio of the DAQ plug-in board ADC sampling frequency to signal (voltage and current) frequency. For sinusoidal input signals the multiplexing delay corresponds to equivalent additive phase shift $\Delta\phi$ between voltage and current. Relative bias caused by this additive phase can be simply derived for sinusoidal current and voltage as

$$\delta_{P\phi} = \frac{P^i - P}{P} = [\cos(\Delta\phi) - (\tan \phi) \cdot \sin(\Delta\phi) - 1] \quad (5)$$

It is depicted as a function of load phase ϕ for four numbers of samples per signal period in Fig. 3.

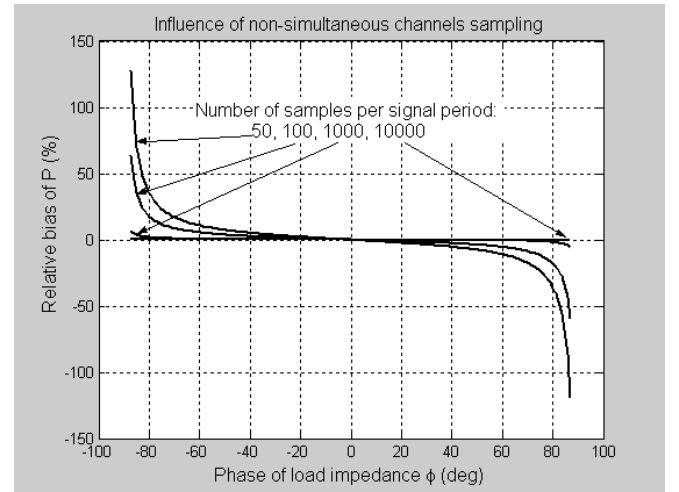


Fig. 3. Bias of active power for rectangular window caused by non-simultaneous sampling

This delay can be compensated using suitable digital filter used to delay the non-delayed channel. The filter should not influence input signal magnitude and should have linear phase with group delay selected so that the delay between input channels is equal to the delay introduced by the filter. Some information about this type of filtering (not applied to measurement of power) is presented e.g. in [7].

A simple compensation method based on linear interpolation (Lagrange interpolation of the first order) was used in our case: Sequence of voltage samples gained at channel one of the DAQ board was before calculation of power replaced by a modified sequence. Each member of the modified sequence is a sum of the original sample and an arithmetic mean of that sample and the consequent sample. This corresponds approximately to the voltage sample that would be gained if both channels were sampled simultaneously in the instants when current input (channel 2) is sampled.

Efficiency of this method depends on the ratio of sampling frequency to the signal frequency and on the position of the processed sample on the sinusoid. Biased caused by multiplexing delay is shown in Fig. 3 and effect of software correction of this bias is shown in Fig. 4.

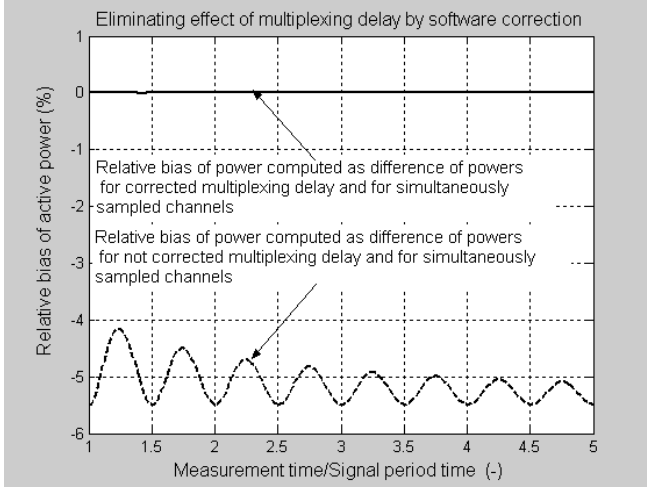


Fig.4 Efficiency of software correction of multiplexing delay; sinusoidal signals, load phase shift $\phi = 60$ deg.

3. INSTANTANEOUS POWER WINDOWING

Bias of active power value shown in Fig. 1 is caused by decimal part of signal period λT_{sig} at the end of T_M . If we multiply the (sampled parts of) signals by a tapering window of the length identical with signal length (as is often done before processing signal in frequency domain), the weight of the part λT_{sig} will be substantially reduced.

The active power corresponding to the *windowed instantaneous power* found from signal samples is

$$P_W = \frac{1}{N} \sum_{n=0}^{N-1} w(n)p(n) \quad (6)$$

where $w(n)$ is the used discrete-time window (identical with samples of the corresponding continuous-time window). Signal windowing causes additional bias, therefore power estimate must be corrected (see (7)).

Since window $w(n)$ is not correlated with $p(n)$, mean value of the $w(n)p(n)$ (i.e. P_W from (6)) is product of mean values of $w(n)$ and $p(n)$. The active power estimate from (1) can therefore be calculated from the values of $w(n)p(n)$ as

$$P' = \frac{\frac{1}{N} \sum_{n=0}^{N-1} w(n)p(n)}{\frac{1}{N} \sum_{n=0}^{N-1} w(n)} = \frac{\sum_{n=0}^{N-1} w(n)p(n)}{\sum_{n=0}^{N-1} w(n)} \quad (7)$$

The most popular windows are the well-known cosine windows defined as

$$w_p(n) = \sum_{i=0}^L a_i \cos\left(\frac{2\pi n i}{N}\right), \quad n = 0, 1, 2, \dots, N-1 \quad (8)$$

where L is window order and N is window length.

The bias of active power found from the windowed instantaneous power using Hann window (a cosine window of the 1st order, $L = 1$, and with coefficients $a_0 = 0.5$, $a_1 = -0.5$) as a function of the normalized time is shown in

Fig. 5 for the same phase shifts of the load that were used in Fig. 1.

The positive influence of windowing on active power bias can be observed when comparing Fig. 1 with e.g. Fig.5. The theoretical formula corresponding to (4) for signal windowing is rather complicated even for Hann window, and it is (meaning of M and λ see (2))

$$\delta_p = \sin(4\pi\lambda)4\pi\lambda \cdot A + \text{tg}\phi \cdot (\cos(4\pi\lambda) - 1) \cdot B$$

$$A = \left[\frac{-1}{4\pi(M+\lambda)} + \frac{1}{8\pi(M+\lambda)+4\pi} + \frac{1}{8\pi(M+\lambda)-4\pi} \right] \quad (9)$$

$$B = \left[\frac{1}{4\pi(M+\lambda)} - \frac{1}{8\pi(M+\lambda)+4\pi} - \frac{1}{8\pi(M+\lambda)-4\pi} \right]$$

Better properties of the active power estimate for non-coherent sampling can be achieved by using higher order windows. Relative bias of active power for Blackman window is shown in Fig.6, for Blackman-Harris minimum four-term (window designed for minimization of side-lobe peaks [2]) is depicted in Fig.7 and Fig.8.

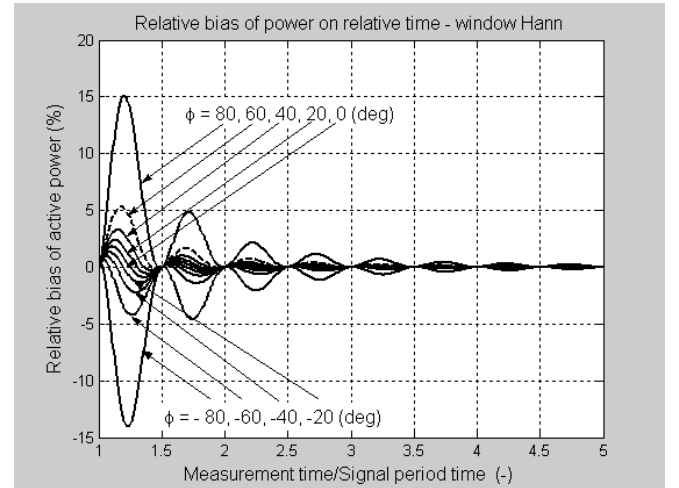


Fig. 5. Bias of active power for window Hann

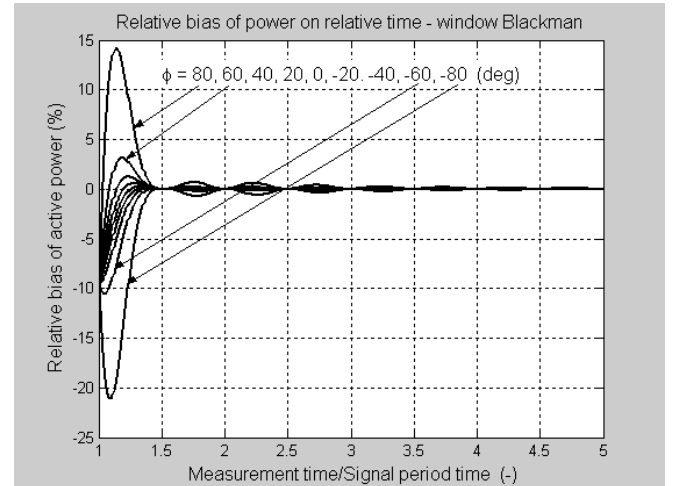


Fig. 6. Bias of active power for window Blackman

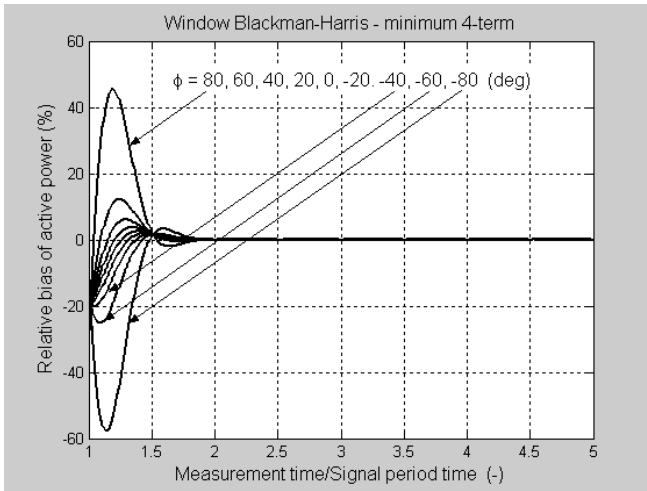


Fig. 7. Bias of active power for window Blackman-Harris, minimum 4-term

Curves in Fig. 5 are again overlapping results of theoretical analysis and numerical simulation. Figures 6 and 7 show efficiency of second-order cosine windows (Blackman and Blackman-Harris, minimum four-term [2]).

Fig. 8 shows slower decrease of active power bias with time if voltage and current signals have non-zero DC components. (compared it to Fig.7, where as in all other figures zero DC parts of voltage and current were supposed).

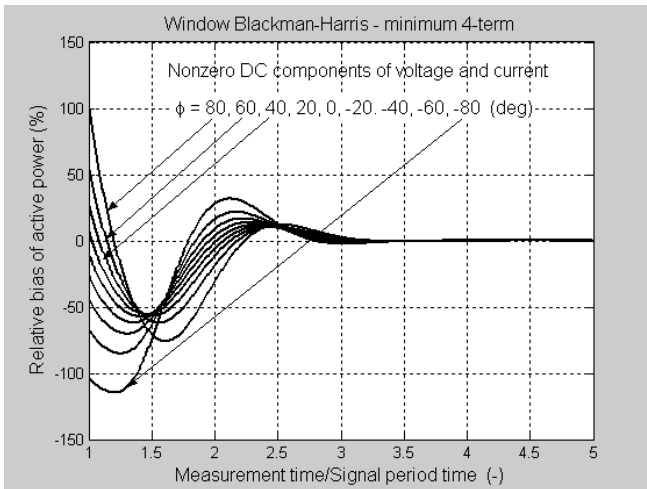


Fig. 8. Bias of active power for window Blackman-Harris, minimum, 4-term; DC components are 50% of voltage and current peak values

Instantaneous power windowing decreases significantly the active power bias. Tab.1 shows how the bias for the various windows depend on number of signal sampled periods. Tab.1 presents values of relative active power bias in percent found as absolute values of local maximums in the bands of $(M + \lambda)$ given in left column and defined by (2).

As can be seen from Tab.1, for increasing number of sampled periods the bias decreases more slowly for Blackman-Harris window than for the remaining ones. This corresponds to slower side-lobes fall-off for Blackman-Harris window spectrum compared to the others.

Tab.1 Effect of windowing on relative active power bias δ_p in percent for several bands of signal periods sampled

$(M+\lambda)$ band	Rectangular window	Hann window	Blackman window	Bl.-Harris window
9 - 10	0.8	$2.3 \cdot 10^{-3}$	$9.4 \cdot 10^{-4}$	$3.5 \cdot 10^{-5}$
99 - 100	0.08	$2.0 \cdot 10^{-6}$	$8.6 \cdot 10^{-7}$	$1.4 \cdot 10^{-5}$
999 - 1000	0.008	$2.0 \cdot 10^{-9}$	$8.5 \cdot 10^{-10}$	$1.4 \cdot 10^{-5}$

We have also examined if using rectangular *rule of numerical integration* should not be replaced by some more complicated integration algorithm. Trapezoidal, Simpson, "3/8" and Newton-Cotes 4th-degree polynomial algorithms were compared by computing active power of sinusoidal signal quantized by 8, 12 and 16-bit ADCs. Differences in errors for using the above enumerated algorithms were negligible, relative bias of active power caused by numerical integration was in the order of 0.1 % for 8-bit quantizing, 0.01 % for 12-bit quantizing and 0.0001 % by 16-bit quantizing.

4. EXAMPLES OF EXPERIMENTAL RESULTS

We have measured the active power using a two-channel generator HP3245A for generation of two sinusoidal signals with defined magnitudes, frequency and phase difference. Signals were digitised by a low-cost multiplexed 12-bit 200 kS/s DAQ plug-in board (6023E of National Instruments). Instruments were controlled by GPIB, MATLAB toolboxes Data Acquisition and Instrument Control were used. The plug-in board multiplexing delay was decreased by means of the algorithm mentioned above.

Examples of measurements are plotted together with simulation results for the same window and the same phase difference of voltage and current in Fig. 9 and Fig. 10. Results of measurement are points denotes as x. Corresponding waveforms are marked in Fig.1 and Fig. 5 as the dashed line. As can be seen the agreement between results of simulation and results of measurement is very good.

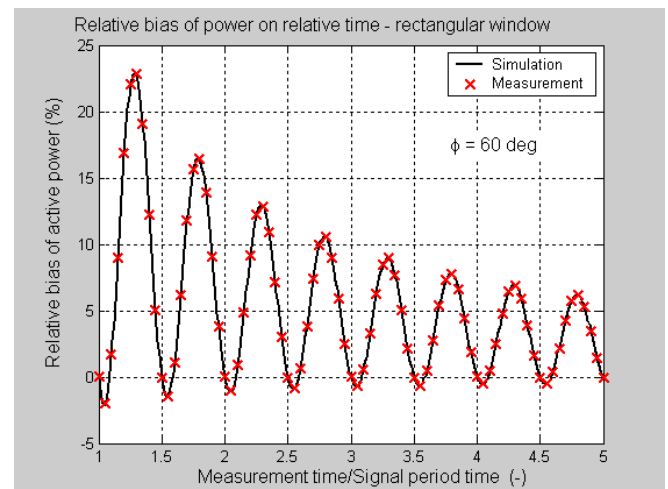


Fig. 9. Bias of active power for rectangular window, load impedance phase $\phi = 60$ deg, simulation and measurement (x)

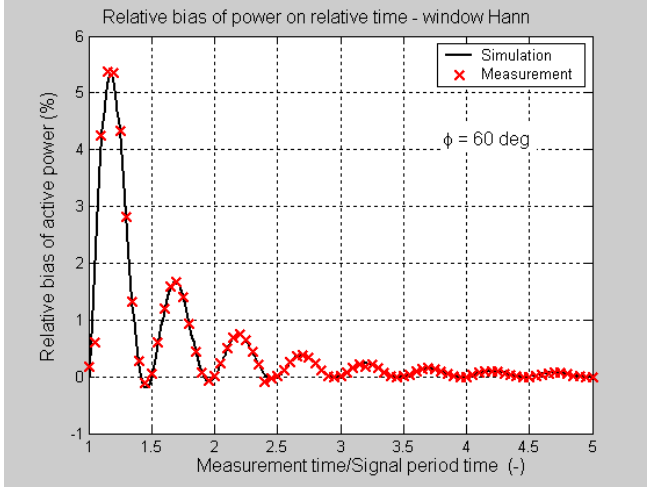


Fig. 10. Bias of active power for window Hann, load impedance phase $\phi = 60$ deg, simulation and measurement (x)

5. MEASUREMENT OF ACTIVE POWER OF NON-SINUSOIDAL SIGNALS

The figures and the formulas above were given for sinusoidal waveforms of voltage and current and for arbitrarily chosen phase difference of voltage and current phasors. In this paragraph we present some results of time-domain active power estimation for a multi-frequency signals and for a given load impedance. The impedance is a series of a resistance and an inductance and the values of these elements were selected so that the impedance magnitude is 1 and its phase is $\pi/4$ at power line (50 Hz) frequency. The magnitudes of higher harmonic components of voltage were selected based on compatibility levels given in international standard [9] (for the THD = 8%).

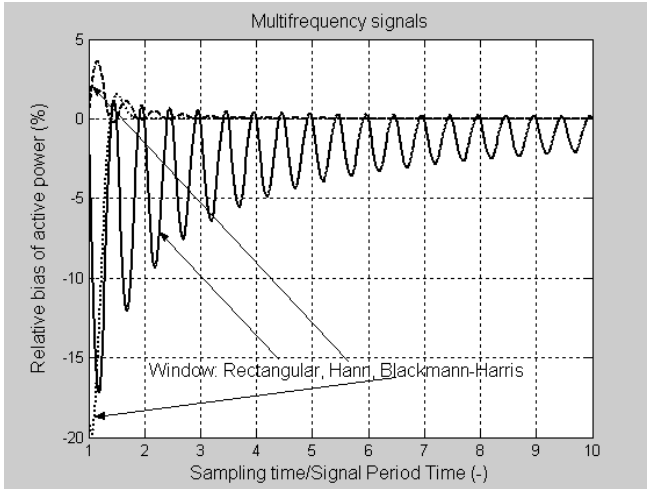


Fig. 11 Decreasing active power bias of multi-harmonic signals caused by non-coherent sampling by windowing

Only three harmonic components (having the largest magnitudes [9]) were used in simulation. The phase of all voltage harmonic components was set to zero (no value is suggested for these phases in [9]).

Tab.2 Higher harmonic components of multi-frequency voltage the power estimates of which are shown in Fig. 11

Order of harmonic	Level (%)
1	100
3	5
5	6
11	3.5

Example of active power estimates for these signals is shown in Fig. 11 Higher harmonic components of voltage used in simulations were those given in Tab.2.

6. UNCERTAINTY OF POWER ESTIMATION DUE TO QUANTIZATION

In the previous text the influence of non-coherent sampling on the bias of active power estimate was introduced. Resultant estimate is also affected by additive noise influencing input signal samples. The most significant component of this additive noise is usually noise due to signal quantization, i.e. quantization noise. Presence of noise leads to uncertainty of the active power estimate. This uncertainty component can be derived by applying the law of uncertainty propagation [10] on (7), taken into account that $p(n) = u(n) \cdot i(n)$. This leads to

$$u^2(P') = \sum_{n=0}^{N-1} \left(\frac{\partial P'}{\partial v(n)} \right)^2 u^2(v(n)) + \sum_{n=0}^{N-1} \left(\frac{\partial P'}{\partial i(n)} \right)^2 u^2(i(n)) \quad (10)$$

$$= ENBW \times (I_{RMS}^2 u_n^2(v) + V_{RMS}^2 u_n^2(i))$$

where V_{RMS} , I_{RMS} are RMS values of voltage and current $v(n)$, $i(n)$ and $u_n(v)$ and $u_n(i)$ are standard deviations of noise affecting input samples $v(n)$ and $i(n)$. $ENBW$ is the equivalent noise bandwidth of the used window [2],

$$ENBW = \frac{\sum_{n=0}^{N-1} w^2(n)}{\left(\sum_{n=0}^{N-1} w(n) \right)^2} \quad (11)$$

If noise is caused mostly by signal quantization then

$$u_n(v) = \frac{V_{range}}{2^{ENOB} \sqrt{12}}, \quad u_n(i) = \frac{I_{range}}{2^{ENOB} \sqrt{12}} \quad (12)$$

where V_{range} and I_{range} are full-scale ranges of voltage channel and current channel and $ENOB$ is effective number of bits of the used ADC.

Since $ENBW$ of all windows is greater than $ENBW$ of rectangular window, the used window slightly increases the active power estimate uncertainty compared to uncertainty of power estimate in case of using rectangular window (see (10) and Tab.3).

Tab.3 Uncertainty of power estimate, measured and theoretical found using (10)

Window	Window order L	Relative uncertainty (%)	
		<i>theoretical</i>	<i>measured</i>
Rectangular	0	$4.7 \cdot 10^{-3}$	$4.2 \cdot 10^{-3}$
Hann	1	$5.8 \cdot 10^{-3}$	$4.6 \cdot 10^{-3}$
Blackman	2	$6.2 \cdot 10^{-3}$	$4.9 \cdot 10^{-3}$
Blackman-Harris 4Term	3	$6.8 \cdot 10^{-3}$	$5.2 \cdot 10^{-3}$

The measured uncertainties in Tab.3 were obtained from measurement using the DAQ plug-in board NI 6023E mentioned above, for 500 measurement repetition. The *ENOB* for 6023E board was measured to be 11.2 bits, measurement was performed for 1000 Sa/period and phase difference 60 deg. The *ENBW* of cosine windows increases with window order, which corresponds to results from Tab.3.

7. CONCLUSION

The described method allows reducing substantially the active power measurement bias for non-coherent sampling, (see Tab.1). Windowing instantaneous power in time domain allows also substantial measurement time reduction compared to classical method without window use (i.e. using rectangular window), which may be important in real-time digital signal processing. Increasing window order leads on one hand to substantial reduction of power estimate bias but on the other hand to slight increase of uncertainty due to input signals quantization. Multiplexing delay caused by using low-cost multiplexed DAQ plug-in boards can be efficiently decreased using a very simple algorithm described in the text.

ACKNOWLEDGMENT

This research was supported by the research program No. MSM6840770015 "Research of Methods and Systems for Measurement of Physical Quantities and Measured Data Processing " of the CTU in Prague sponsored by the Ministry of Education, Youth and Sports of the Czech Republic.

REFERENCES

- [1] A.Ferrero, R. Ottoboni, J.H., "High-Accuracy Fourier Analysis Based on Synchronous Sampling Techniques," IEEE Transactions on Instrumentation and Measurement, Vol. 41, No. 6, pp.780-785, December 1992
- [2] F. J. Harris, "On the use of windows for harmonic analysis with discrete Fourier transform", Proc. IEEE, vol.66, pp.51-83, 1978
- [3] J. Schoukens, R. Pintelon, H. V. Hamme, "The Interpolated Fast Fourier Transform: A Comparative Study", IEEE Transactions on Instrumentation and Measurement, vol. 41, no.2, pp. 226-232, April 1992
- [4] G. Andria, M. Savino, A. Trotta, "Windows and interpolation algorithms to improve electrical measurement accuracy", IEEE

Transactions on Instrumentation and Measurement, vol. 38, no.4, pp.856-863, August 1989.

- [5] M. Sedláček, M. Titěra, "Interpolations in frequency domains used in FFT spectrum analysis", Measurement, vol 23, no. 3, pp. 185-193, April 1998.
- [6] D. Agrez, "Active Power Estimation in the Non-coherent Sampling: A Comparative Study," Proceedings of the IMTC 2005 – Instrumentation and Measurement Technology Conference, Ottawa, Canada, May 2005, pp. 720-725
- [7] A. Barwicz, D. Bellemare, R. Z. Morawski, "Digital Correction of A/D Conversion Error Due to Multiplexing Delay", IEEE Transactions on Instrumentation and Measurement, Vol. 39, No. 1, pp.76-79, February 1990
- [8] O. M. Solomon, "The Use of Windows in Signal-to-Noise Ratio and Harmonic Distortion Computations, IEEE Transactions on Instrumentation and Measurement, Vol. 43, No. 2, pp.194-199, April 1994
- [9] IEC 61000-2-2, Electromagnetic Compatibility, Part.2 – Environment, Section 2: Compatibility levels for low-frequency conducted disturbances and signalling in public low-voltage power supply systems. IEC, Switzerland, 1990
- [10] Guide to Expression of Uncertainty in Measurements, International Organization for Standardization, Switzerland, 1993